



This is a self-archived – parallel published version of an original article. This version may differ from the original in pagination and typographic details. When using please cite the original.

Riemer H.J.A. Slart, Frank M. Bengel, Cigdem Akincioglu, Jamieson M. Bourque, Wengen Chen, Marc R. Dweck, Marcus Hacker, Saurabh Malhotra, Edward J. Miller, Matthieu Pelletier-Galarneau, René R.S. Packard, Thomas H. Schindler, Richard L. Weinberg, Antti Saraste, Piotr J. Slomka. Total-Body PET/CT Applications in Cardiovascular Diseases: A Perspective Document of the SNMMI Cardiovascular Council *J Nucl Med.* 2024; 65 (4); 607-616; DOI: <https://doi.org/10.2967/jnumed.123.266858> © SNMMI.

Total-Body PET/CT Applications in Cardiovascular Diseases: A Perspective Document of the SNMMI Cardiovascular Council

Riemer H.J.A. Slart^{1,2}, Frank M. Bengel³, Cigdem Akincioglu⁴, Jamieson M. Bourque⁵, Wengen Chen⁶, Marc R. Dweck⁷, Marcus Hacker⁸, Saurabh Malhotra⁹, Edward J. Miller¹⁰, Matthieu Pelletier-Galarneau¹¹, René R.S. Packard¹², Thomas H. Schindler¹³, Richard L. Weinberg¹⁴, Antti Saraste¹⁵, and Piotr J. Slomka¹⁶

¹Medical Imaging Centre, Department of Nuclear Medicine and Molecular Imaging, University Medical Center Groningen, University of Groningen, Groningen, The Netherlands; ²Biomedical Photonic Imaging Group, Faculty of Science and Technology, University of Twente, Enschede, The Netherlands; ³Department of Nuclear Medicine, Hannover Medical School, Hannover, Germany; ⁴Division of Nuclear Medicine, Medical Imaging, Western University, London, Ontario, Canada; ⁵Departments of Medicine (Cardiology) and Radiology, University of Virginia, Charlottesville, Virginia; ⁶Department of Diagnostic Radiology and Nuclear Medicine, University of Maryland School of Medicine, Baltimore, Maryland; ⁷British Heart Foundation Centre for Cardiovascular Science, Edinburgh Heart Centre, University of Edinburgh, Edinburgh, United Kingdom; ⁸Division of Nuclear Medicine, Department of Biomedical Imaging and Image-Guided Therapy, Medical University of Vienna, Vienna, Austria; ⁹Cook County Health, Rush Medical College, Chicago, Illinois; ¹⁰Department of Biomedical Engineering, Yale University, New Haven, Connecticut; Department of Radiology and Biomedical Imaging, Yale School of Medicine, and Department of Internal Medicine, Yale University, New Haven, Connecticut; ¹¹Department of Medical Imaging, Montreal Heart Institute, Montreal, Quebec, Canada; ¹²Division of Cardiology, Department of Medicine, David Geffen School of Medicine, UCLA, Los Angeles, California; ¹³Mallinckrodt Institute of Radiology, Division of Nuclear Medicine, Cardiovascular Medicine, Washington University School of Medicine, St. Louis, Missouri; ¹⁴Division of Cardiology, Feinberg School of Medicine, Northwestern University, Chicago, Illinois; ¹⁵Turku PET Centre and Heart Center, Turku University Hospital and University of Turku, Turku, Finland; and ¹⁶Division of Artificial Intelligence in Medicine, Department of Medicine, Cedars-Sinai Medical Center, Los Angeles, California

Digital PET/CT systems with a long axial field of view have become available and are emerging as the current state of the art. These new camera systems provide wider anatomic coverage, leading to major increases in system sensitivity. Preliminary results have demonstrated improvements in image quality and quantification, as well as substantial advantages in tracer kinetic modeling from dynamic imaging. These systems also potentially allow for low-dose examinations and major reductions in acquisition time. Thereby, they hold great promise to improve PET-based interrogation of cardiac physiology and biology. Additionally, the whole-body coverage enables simultaneous assessment of multiple organs and the large vascular structures of the body, opening new opportunities for imaging systemic mechanisms, disorders, or treatments and their interactions with the cardiovascular system as a whole. The aim of this perspective document is to debate the potential applications, challenges, opportunities, and remaining challenges of applying PET/CT with a long axial field of view to the field of cardiovascular disease.

Key Words: long axial field-of-view PET/CT; cardiovascular diseases; current status; future perspectives

J Nucl Med 2024; 65:607–616
DOI: 10.2967/jnumed.123.266858

Recently, digital PET/CT systems with a long axial field of view (LAFOV) have become available as the current state-of-the-art clinical imaging systems. These new camera systems enable a larger anatomic coverage and a significant increase in system sensitivity, with a factor of 10–40, depending on the volume of detector material, that is, the actual length of the scanner (1,2). This is due to the numerous, highly performing silicon photomultiplier-based detectors collecting a huge number of coincidence photons, with consequent improvement of signal-to-noise ratio that, in turn, positively impacts image quality. Preliminary results from the clinical application of LAFOV systems therefore demonstrate improved image quality and lesion quantification (1,3). Low-dose examination protocols and a significant reduction in acquisition time are other potential advantages. These novel scanners also allow quantitative dynamic imaging of the whole body with high temporal resolution in a large field of view (4). The whole-body coverage enables simultaneous assessment of multiple organs and large vascular structures, opening new opportunities for imaging cardiovascular disorders.

The aim of this perspective is to discuss the potential applications, opportunities, and challenges of LAFOV PET/CT in the field of cardiovascular disease (CVD).

MULTIORGAN APPROACH IN CARDIOVASCULAR DISORDERS

Driven by the results of an increasing number of clinical trials, cardiovascular medicine is changing and moving beyond a single-organ-centered approach. Contemporary optimal cardiovascular care focuses on the whole body and includes a systems-based

Received Nov. 7, 2023; revision accepted Jan. 11, 2024.
For correspondence or reprints, contact Riemer Slart (r.h.j.a.slart@umcg.nl).
Published online Feb. 22, 2024.
COPYRIGHT © 2024 by the Society of Nuclear Medicine and Molecular Imaging.

approach in which the heart and circulatory system are embedded in integrated networks (Fig. 1). Despite symptom improvement in chronic coronary syndromes, targeted coronary artery revascularization may not improve patient survival even in the presence of myocardial ischemia (5). On the other hand, systemic medical therapy does improve CVD outcomes, and this includes targeted modulation of the neurohumoral, endocrine, and immune systems (6,7). Likewise, the interplay between heart, vessel wall, and other organs is increasingly emphasized for optimal cardiovascular health. Based on different organ and system interactions, various subdisciplines such as cardioimmunology (8), cardioneurology (9), or cardiooncology (10) have emerged, and the cardiorenal (11), cardiohepatic (12), cardiopulmonary, and gut–heart axes (13,14) are being explored to obtain mechanistic insights and identify therapeutically exploitable targets. Accordingly, diagnostic imaging tests, which provide information about the entire body, may be of significant value. Hence, LAFOV PET/CT may provide the diagnostic armamentarium for high-quality, innovative cardiovascular medicine within the overall context of systems medicine.

METHODOLOGY CONCERNING LAFOV PET

Hot-spot cardiovascular PET data are mainly presented by way of weight, activity, and SUV maps, which physicians are trained to interpret in a qualitative and subjective way. The shortcomings of SUV are well known (Table 1). In contrast, there are established and quantitative methods for the analysis of dynamic PET data, which can reveal deeper insights into physiologic parameters that are not possible to measure from single-time-point SUV analysis. Clear benefits to this approach, such as improved lesion detection due to parametric imaging (15), could be very helpful in imaging CVDs, particularly for smaller lesions such as those in atherosclerosis.

Further, the large amount of data generated by total-body scanners, and the consequently long reconstruction times (Fig. 1), necessitate high-performance hardware to prevent the need for transferring these datasets over traditional hospital information technology networking systems. Nonetheless, the acquired data offer a wealth of additional information that can be extracted using both conventional methods of mathematical modeling and artificial intelligence. The use of population-based input functions with shorter dynamic ^{18}F -FDG protocols in a LAFOV PET/CT system is a good example of this, decreasing acquisition time from 60 to 10 min (4). Further, artificial intelligence is expected to play an increasingly critical role in imaging equipment, reconstruction, and postprocessing pipelines in the field of nuclear medicine (16) and likely to have value in LAFOV PET/CT due to its capacity to

process and learn from large amounts of data (Fig. 1). Novel deep-learning reconstruction methods may be used to accelerate the process and improve the image quality. Multiorgan artificial intelligence–based segmentation tools will likely aid in the kinetic modeling of cardiovascular data across the entire patient body.

CARDIOVASCULAR APPLICATIONS

Whole-Body PET Perfusion and Myocardial Blood Flow Quantification

PET/CT has become a mainstay in the detection and characterization of subclinical and clinically manifested coronary artery disease (CAD) (17) and for viability assessments in ischemic cardiomyopathy (18). PET remains the noninvasive gold standard for quantification of myocardial blood flow and cerebral blood flow. Because of the presence of the blood–brain barrier, PET measurements of cerebral blood flow are mostly conducted with the radiotracer ^{15}O - H_2O (19–21). In the heart, clinical blood flow quantification relies on various radiotracers such as ^{82}Rb -Cl, ^{13}N - NH_3 , ^{15}O - H_2O , and (in the future) ^{18}F -flurpiridaz (22). Myocardial blood flow quantification has well-established clinical applications in epicardial CAD and coronary microvascular dysfunction (23,24). Studies have demonstrated the feasibility of measuring blood flow in specific organs, such as the kidneys with ^{15}O - H_2O (25,26), ^{82}Rb -Cl (27,28), and ^{13}N - NH_3 (29). Furthermore, skeletal muscle and splenic blood flow can be measured with PET using ^{15}O - H_2O and ^{82}Rb -Cl (30–34). There are challenges in the evaluation of blood flow at the whole-body level, such as a wide range of flow levels and variable tracer extraction in different organs. Furthermore, there is more than one input in some organs, such as the lungs and the liver. Initial experiences have been obtained with tracers with high extraction, including ^{15}O - H_2O (Fig. 2) and ^{11}C -butanol (35).

With the recent introduction of LAFOV PET/CT, the comprehensive assessment of multiorgan function related to the cardiovascular system appears feasible, opening new avenues and opportunities in research and clinical care. For example, microvascular disease may be determined in virtually all vascular beds concurrently or nearly concurrently, depending on the differences in local radiotracer extraction and tissue kinetics. The dimensionality of the target organs assessed—whole organ, major arterial bed, or segmental arterial bed—may require nuanced evaluations to unmask focal abnormalities in blood flow (36).

Many CVD entities are connected to systemic factors such as the immune and neurohumoral systems and endocrine disorders and may need a more comprehensive and systems-based diagnostic and medical treatment approach (8–14). For example, impaired renal perfusion

contributes to cardiorenal syndrome in heart failure, and there is a need for markers that balance the benefits of the renin–angiotensin–aldosterone system blockade and potential adverse effects related to a decreasing glomerular filtration rate in those with significant kidney disease (11). There is only limited information on myocardial blood flow responses in the lower extremities in atherosclerotic CVD and the value of perfusion imaging in monitoring treatment of critical limb ischemia (37). Data from the REACH registry showed that approximately 10% of patients with CAD present with concomitant peripheral artery disease,

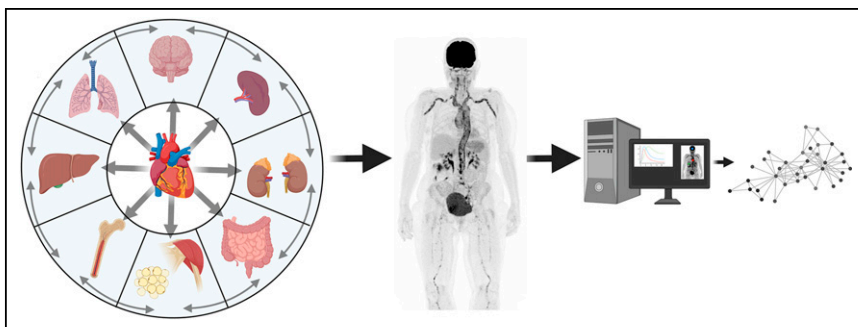


FIGURE 1. Simultaneous cardiovascular multisystem studies with total-body PET and dedicated analysis of dynamic PET data. Arrows in wheel display heart–organ connections and interactions.

TABLE 1

Strengths, Weaknesses, Opportunities, and Threat Analysis of LAFOV Total-Body PET/CT in Cardiovascular Imaging

| Parameter | Description |
|---------------|---|
| Strengths | Whole-body coverage |
| | High spatial and temporal resolution |
| | Dynamic imaging |
| | Short imaging time |
| Opportunities | Low radiation dose |
| | New development in medical imaging |
| | Clinical cardiovascular trials |
| | Biodistribution of newly developed (radiolabeled) cardiovascular drugs |
| Weaknesses | Insights of cardiovascular and multiorgan interaction/cross-talk |
| | Artificial intelligence implementation |
| | CT for attenuation correction, as significant limit to dose reduction (although ultra-low-dose CT, time-of-flight correction, or deep-learning approach will be implemented soon) |
| | Requirement for accurate motion correction |
| Threats | Data storage and networking infrastructure |
| | Lack of easy-to-use clinical kinetic software programs |
| | Number of patient preparation rooms |
| | Costs |
| | Not widely available |
| | Computational times for reconstruction, data corrections, and kinetic modeling |

whereas 60% of patients with peripheral artery disease present with concomitant CAD (38). Data from large randomized clinical trials consistently showed that the coexistence of CAD and peripheral artery disease is a particularly harmful association, with a heightened risk of major adverse cardiovascular events, including myocardial infarction, stroke, and cardiovascular death, compared with

CAD or PAD only (39). Open questions are if functional total-body PET perfusion may resolve the clinical observation that some patients have coronary atherosclerotic disease only, whereas others have systemic vascular disease and still others have both. Do we need to focus directly on vascular atherosclerotic activity? In this respect, the LAFOV PET/CT scanner may afford unique and noninvasive insights in the detection and characterization of cardiovascular physiology and metabolism in conjunction with other organs and systemic factors and may result in the development and monitoring of new treatments.

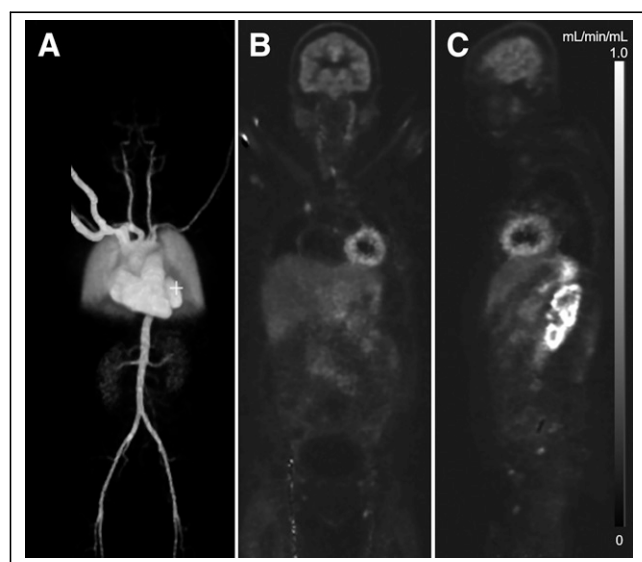


FIGURE 2. Dynamic perfusion imaging with $^{15}\text{O}\text{-H}_2\text{O}$ with Biograph Vision Quadra system (Siemens) and whole-body PET. (A) 3-dimensional parametric image of arterial blood volume (V_a). (B and C) Parametric images of organ-specific blood flow (k_1 , mL/min/mL) in horizontal and sagittal planes, respectively. Images centered in left ventricle show that high flow can be seen in myocardium and kidney.

Atherosclerosis

It remains poorly understood how inflammatory atherosclerotic processes interact in the different vascular beds (e.g., coronary arteries, carotids, aortic arch, peripheral vessels) and with other organ systems (e.g., the brain, gut, hematopoietic tissues). Such systemic interrelations and disease networks could be further determined with LAFOV PET/CT imaging (Fig. 3). Furthermore,

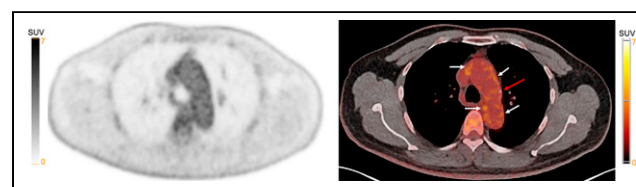


FIGURE 3. $^{18}\text{F}\text{-FDG}$ PET/CT of 56-y-old man 3 mo after successful revascularization of acute myocardial infarction. Images were obtained using LAFOV PET/CT (Siemens Vision Quadra) 60 min after injection. $^{18}\text{F}\text{-FDG}$ PET (left) and PET/CT (right) images were acquired with high sensitivity and spatial resolution, enabling detection of slightly increased spotty FDG accumulation in arterial wall of aortic arch (white arrows), with only 1 calcified focus (red arrow) indicating increased inflammatory atherosclerotic activity in otherwise less advanced atherosclerotic stage.

ultralow radiation dosing makes multiple-time-point and sequential multitracer studies increasingly feasible. These features are of particular interest in atherosclerosis, which is a systemic condition that changes with time and treatment and involves different pathologic processes including inflammation, calcification, fibrosis, and thrombus formation. Each of them can be targeted with modern PET tracers. For example, ^{18}F -FDG PET has already been used to investigate how large vessel inflammation (aorta) is increased after myocardial infarction and is linked with increases in psychologic stress (amygdala of the brain) and hematopoietic bone marrow activity (40). Multitracer studies could be used to investigate how vascular inflammation associates with calcification activity (^{18}F -fluoride) (41), fibroblast activation (^{68}Ga -fibroblast activation protein inhibitor [FAPI]) (42,43), and thrombus formation (^{18}F -glycoprotein 1) (44).

Dynamic total-body ^{18}F -FDG images yield a high vessel wall signal and target-to-background ratio, even after several half-life times of decay, allowing the cross-talk between vessel wall and lymphoid organs to be identified, including parametric imaging of metabolic rate of ^{18}F -FDG (45). Novel and inexpensive radiopharmaceuticals with higher patient throughput may hold promise in advancing our understanding of atherosclerosis as well as a range of other cardiovascular conditions and in improving patient assessment and treatment.

Myocardial and Peripheral Muscular Metabolism

A variety of radiotracers informs cardiac metabolism. ^{18}F -FDG is a glucose analog, of which uptake provides a surrogate for glucose metabolism in cardiac myocytes. Radiolabeled long-chain fatty acids and fatty acid analogs, such as ^{11}C -palmitate and ^{18}F -fluoroheptadecanoic acid, allow imaging of fatty acid metabolism, including oxidation and lipid storage (46,47). Oxidative metabolism can be evaluated with ^{11}C -acetate, in which washout reflects myocardial oxygen consumption (48,49).

Studies using metabolic PET tracers have shown distinct alterations in myocardial substrate metabolism and external efficiency in various cardiac diseases including heart failure (49,50). These relate partially to alterations in systemic metabolism, such as those that occur in obesity and diabetes (51). By assessing the metabolism simultaneously in multiple organs, including the heart, skeletal muscles, liver, and adipose tissue, LAFOV PET can contribute to studying organ-specific changes in cardiometabolic diseases and related cardiovascular complications (52). For example, cardiac and systemic insulin resistance is a typical feature of heart failure that predicts impaired functional capacity and reduced survival (53). However, mechanisms of insulin resistance differ between cardiac and skeletal muscle related to substrate metabolism and hemodynamic stressors (54). Metabolic imaging with LAFOV PET/CT may provide answers to the associations between myocardial and peripheral insulin resistance in cardiac disease and diabetes (55). Given its superior sensitivity, accurate modeling of multiple compartments in dynamic datasets may become possible to derive new insights into glucose, fatty acid, and oxidative metabolism (56). Such an approach has been demonstrated previously to determine the influx rate, fractional blood volume, tracer delivery rate, and volume of distribution of ^{18}F -FDG in tumors (56) and in patients recovering from coronavirus disease 2019 infection (57).

Involvement of the Heart in Systemic Disease

Sarcoidosis is a multisystem inflammatory condition of unknown etiology and predominantly affects the lungs and lymph nodes;

cardiac sarcoidosis is clinically apparent in 5%–10% of patients, and it is the most frequent cause of death in these patients (58,59). Autopsy data demonstrate cardiac sarcoidosis involvement in 25% of cases, suggesting that many patients with cardiac sarcoidosis are not recognized with current imaging techniques.

^{18}F -FDG PET is currently recommended for the assessment of patients with suspected cardiac sarcoidosis (60) and is characterized by intense focal uptake in the myocardium, which corresponds with areas of myocardial injury observed either on rest perfusion nuclear imaging or late gadolinium enhancement sequences from cardiovascular MRI (61). This finding provides important prognostic information (62) and frequently prompts the prescription of anti-inflammatory agents and consideration of (expensive) cardiac device implantation.

LAFOV PET/CT would potentially improve our assessment of patients with cardiac sarcoidosis, allowing us to better appreciate sarcoidosis involvement across multiple organs (e.g., brain, heart, lungs, gut, skin, eyes, lymph nodes). Given the low sensitivity of myocardial biopsy, histologic proof of extracardiac sarcoidosis guided by imaging findings can also be valuable for diagnosis of cardiac sarcoidosis (60). Reduced radiation doses are particularly attractive when considering longitudinal imaging to track disease progression and response to therapy (60).

Cardiac amyloidosis is part of a systemic disease in which amyloidogenic proteins deposit in target organs, leading to dysfunction. There are 2 major types of cardiac amyloidosis: transthyretin amyloidosis and amyloidosis where the amyloidogenic proteins are either misfolded transthyretin or misfolded immunoglobulin light chains (amyloid light-chain amyloidosis) (63). Over the past decade, imaging of cardiac amyloidosis has undergone a revolution with the adoption of bone scintigraphy imaging using SPECT tracers and techniques that have allowed for the noninvasive diagnosis of transthyretin cardiac amyloidosis. However, there are also multiple unmet needs in the evaluation of amyloidosis that lend themselves to the use of PET-based radiotracers, including quantification of total-body or target organ amyloid disease burden, differentiation between various types of amyloidosis, and determination of treatment response.

By the nature of PET imaging, PET-based radiotracers are more quantitative than their SPECT counterparts. Parametric imaging with PET can be a valuable tool for the quantification of PET tracer uptake (64). Therefore, the use of PET imaging for evaluation of cardiac amyloidosis is most likely to center around the qualitative nature of this modality. Four thioflavin analog PET tracers have shown promise for the diagnosis of cardiac amyloidosis. These include ^{11}C -labeled Pittsburgh compound B, ^{18}F -florbetapir, ^{18}F -florbetaben, and ^{18}F -flutemetamol (65). There are data from these agents that have shown preliminary utility in imaging the heart, including kinetic modeling (66,67), whole-body or cardiac disease burden (68–70), and amyloid isotype differentiation (71). There is also interest in the use of the bone tracer ^{18}F -NaF for imaging transthyretin cardiac amyloidosis (72).

The use of whole-body PET systems may allow for more accurate and earlier diagnosis of cardiac involvement while simultaneously offering the ability to determine the total systemic disease burden, including dynamic and parametric image quantification. Whole-body PET systems could allow for determination of total-body disease burden in response to therapy, which is of particular interest in amyloid light-chain amyloidosis, where various target organs (heart, gastrointestinal tract/liver, kidneys) can be involved and would normally require longer, multiple-bed-position acquisitions with traditional

PET machines. Unlike amyloid light-chain amyloidosis, the role of circulating biomarkers (natriuretic peptides, transthyretin, RNA polymerase II subunit B4) in the diagnosis and management of transthyretin cardiac amyloidosis is much less defined and validated (73). The availability of disease-modifying agents highlights the need for new markers capable of addressing correct clinical management and more accurate prognostic stratification (73). Markers define the minimum disease threshold to justify starting new treatments and to exclude patients with infiltration so advanced that they would not benefit from therapy or to identify “responders” and “nonresponders” to a specific disease-modifying agent. LAFOV PET/CT could therefore potentially provide new markers of cardiac involvement relative to total-body disease burden and will be relevant in systemic diseases such as amyloidosis.

Large vessel vasculitis (LVV) disorders are defined as chronic inflammatory disorders that affect the arteries, with variants distinguished in giant cell arteritis, Takayasu arteritis, and isolated (noninfectious) aortitis. These often present with nonspecific constitutional symptoms, which make an accurate diagnosis challenging. Timely diagnosis is of the utmost importance to initiate appropriate treatment and to avoid potential life-threatening vascular (stenosis, dilation, rupture) and potential multiorgan complications (74). ^{18}F -FDG PET/CT is now widely accepted as a useful tool to aid in the diagnosis of LVV and is included in current guideline recommendations (75,76). The increased sensitivity of LAFOV PET/CT may provide added value in detecting suppressed arterial wall ^{18}F -FDG PET activity due to glucocorticosteroid use (77) or unclear cases where residual or reactivated LVV activity is suspected (Fig. 4). The ability to perform low-dose radiation imaging or short-duration scans is also attractive, particularly when considering the need for repeat imaging in patients. The use of appropriate (multiorgan/vascular) kinetic models will provide a significantly higher target-to-background ratio than is possible with conventional scoring and quantification (2,78). Dynamic PET angiography can even be reconstructed from early dynamic PET/CT images for the evaluation of arteries, of particular interest as a one-stop-shop approach in LVV (79), or may include the use of specific inflammatory tracers with dynamic PET (80). The main challenge with systemic vasculitis is the differentiation from widespread atherosclerosis, given the important role inflammation plays in the pathogenesis of atherosclerosis (81) and the difficulty differentiating between active and nonactive LVV (smoldering disease) during and after therapy (82). Visual differentiation is mainly based on pattern. A pattern that is more heterogeneous (83) could further characterize differences in a more precise and less reader-dependent method and may be further improved with specific PET-labeled markers for assessment of remaining LVV activity (82). In general, autoimmune diseases are vast, and many are understudied in cardiovascular risk. Various immunotherapies affect the cardiovascular system, and cardiovascular risk in the field of cardiorheumatology is still unknown (83). A crucial area of scientific investigation is moving forward in which LAFOV PET/CT can play a central role.

Heart failure with preserved ejection fraction (HFpEF) is increasing in prevalence worldwide, already accounting for at least half of all heart failure. Recently, strong evidence for bidirectional crosstalk between metabolic stress and chronic inflammation has emerged, and alterations in systemic and cardiac immune responses are held to participate in HFpEF pathophysiology (84). Given the well-established heterogeneity among HFpEF phenotypes, coupled with the robust complexity and intertwined interactions between metabolic events and inflammation, a comprehensive program of



FIGURE 4. LAFOV ^{18}F -FDG PET/CT in 55-y-old woman with active large vessel giant cell arteritis and moderate progressive muscle relaxation activity at shoulders and hips. PET acquisition time was 4 min.

investigation will be required. LAFOV PET/CT may unravel meta-inflammatory mechanisms contributing to HFpEF pathophysiology and evaluate the systemic effect of new therapeutic (anti-inflammatory) approaches (84).

Autonomic Nervous System

Using various radiolabeled catecholamines or catecholamine analogs, PET has been successfully applied for interrogation of the cardiac sympathetic nervous system. Global and regional impairments of myocardial innervation have been identified in heart failure, ischemic and structural heart disease, various cardiomyopathies, and systemic diseases affecting the heart, such as diabetes mellitus, amyloidosis, and Parkinson disease (85,86). Of note, a prognostic value has been established in heart failure, where the severity of innervation impairment is an independent predictor of adverse events, including arrhythmias (85,87,88). Among patients with ischemic cardiomyopathy, the severity of myocardial sympathetic denervation measured on ^{11}C -hydroxyephedrine PET has an established prognostic value for adverse cardiovascular events, including malignant ventricular arrhythmias (72,74,75). Similar clinical applications are being sought from ^{18}F -flubenguane or ^{18}F -LMI1195, which will support greater application of myocardial denervation on PET (89,90). Although a clear-cut clinical indication

has not yet been established for PET imaging of cardiac innervation, it has certainly provided profound mechanistic insights into the interaction between myocardial catecholamine handling, contractile function, electrophysiology, and other pathophysiologic mechanisms in various cardiac diseases (91). LAFOV PET/CT now provides the opportunity to expand these mechanistic insights by putting cardiac innervation into the framework of total-body catecholamine handling and by providing information about the simultaneous state of other networking organs. For example, experimental studies have suggested that sympathetic stimulation of hematopoietic organs plays a role in immune-mediated progression of CVD (92), whereas richly innervated brown fat may attenuate catecholamine-mediated heart failure progression (93). A comprehensive LAFOV total-body PET protocol, which covers catecholamine kinetics sensitively and simultaneously in all relevant organs and considers the effects of circulating catecholamine levels (94) and the role of nonspecific tracer signal from some tissues (95), may provide answers to questions regarding the interaction between the heart, the autonomic nervous system, and other systems in health and disease. Meta-¹⁸F-fluorobenzylguanidine, an analog of meta-iodobenzylguanidine, was recently used to study myocardial sympathetic innervation and was noted to exhibit rapid and sustained uptake in the myocardium (96). Although dynamic meta-¹⁸F-fluorobenzylguanidine PET allows for quantitation of its volume of distribution, which is a surrogate for norepinephrine transporter-1 density in the myocardium, a LAFOV PET/CT approach would quantitate autonomic function at a more systemic level. Finally, sensory neurons detect invading pathogens and immune cell activation and, in response, relay signals to the central nervous system and act locally to regulate immune cell function. Most exciting are the possibilities of translating our understanding of these neuroimmune communications to new therapies in the cardiovascular field and linking organs, especially given the possibility of repurposing the neuron-specific pharmacologic agents that have already been developed (97).

Cardiovascular Infections

The dramatic recent increase in implantation of prosthetic valves, cardiac implantable electronic devices, vascular grafts, and ventricular assist devices has led to a rise in cardiovascular infections with associated high morbidity and mortality and substantial health costs (98–100). Accurate diagnosis of cardiovascular infection is challenging. Echocardiography and CT play an important role but have limitations, including acoustic shadowing, metal artifacts, and reduced specificity from noninfected vegetations (101–103). ¹⁸F-FDG PET/CT allows earlier diagnosis before extensive morphologic damage, as well as the detection of remote septic emboli and other noncardiac manifestations (104). These advantages improve diagnostic accuracy to a high level, with metaanalyses showing 73%–100% sensitivity and 71%–100% specificity for prosthetic valve endocarditis and 87% sensitivity and 94% specificity for cardiac implantable electronic device infection (105,106). In suspected left ventricular assist device infection, ¹⁸F-FDG PET/CT can localize the site of infection with a prognostic value (107).

LAFOV PET/CT is an emerging tool with advantages that may counteract existing ¹⁸F-FDG PET/CT limitations. Full-body coverage and greater signal-to-noise ratio with total-body PET/CT may help detect smaller and low-grade ¹⁸F-FDG-avid septic foci, even in the young (Fig. 5) (108). LAFOV PET/CT also covers multiple organ systems, including bone marrow, spleen, and lymph node stations that can be involved in cardiovascular infections. In patients with high ¹⁸F-FDG uptake in the bone marrow, a cardiovascular or

musculoskeletal focus of infection is more likely, typically with gram-negative species. A cardiovascular focus of infection is also more likely in the setting of high splenic ¹⁸F-FDG uptake (109). A significant challenge for ¹⁸F-FDG PET/CT in evaluation of cardiovascular device infection is distinguishing between infection and nonspecific inflammation, particularly in the early postoperative setting or with bioadhesive use (110,111). Distinct pharmacokinetic patterns of ¹⁸F-FDG uptake on dynamic-imaging LAFOV PET/CT may help differentiate foci of infection from inflammation.

Development of novel non-¹⁸F-FDG PET tracers that exhibit direct binding to bacteria may direct imaging of infection rather than inflammation as a surrogate. For example, ¹⁸F-labeled polysaccharides that target bacteria-specific maltodextrin transporter (¹⁸F-sorbitol, ¹⁸F-maltohexaose, ¹⁸F-maltose, ¹⁸F-maltotriose) achieve a high intrabacterial activity due to continuous internalization, facilitating infection imaging with high sensitivity. Other non-¹⁸F-FDG infection imaging tracers include radiolabeled antibiotics, antimicrobial peptides, bacterial antibodies, bacteriophages, and bacterial DNA/RNA hybrid nucleotide oligomers (112). Nevertheless, these tracers encounter low sensitivity due to bacterial surface binding only, without intrabacterial signal amplification. The high sensitivity of LAFOV PET/CT may allow direct visualization of these bacteria-binding tracers despite a low signal.

RADIOPHARMACEUTICALS AND DRUG DEVELOPMENT

LAFOV PET/CT scanners have exhibited the ability to enhance clinical diagnostics by enabling imaging at delayed time points after injection. This delayed imaging approach holds promise not only for clinical applications but also for advancing research endeavors through improved characterization of tracer biology. Notably, extending imaging to as late as 24 h after injection of a standard ¹⁸F-FDG dose has revealed a more pronounced washout of tracer from the circulating blood pool, concomitant with heightened uptake in cardiovascular tissue. Furthermore, using images of the newly introduced long-lived ⁸⁹Zr-labeled anti-CD8 minibody against T cell CD8+ at the 24-h mark unveiled the potential to longitudinally monitor immune cell (slower) dynamics. This novel application could potentially find utility in cardiovascular imaging, particularly in atherosclerosis research (113).

An illustrative instance involves ⁶⁸Ga- or the longer-lasting ⁶⁴Cu-labeled DOTATATE, a Food and Drug Administration–approved PET radiotracer known for its binding to somatostatin receptor type 2, primarily used for identifying and tracking somatostatin receptor type 2–positive neuroendocrine tumors. Importantly, this radiotracer is gaining rapid traction in the realm of cardiovascular inflammation imaging (114). Further, PET radiotracers targeting fibroblast-activation protein are now being evaluated increasingly beyond oncologic imaging, such as in the heart, where stimuli activate fibroblasts, leading to progressing interstitial fibrosis and resulting in cardiac dysfunction. Recent literature has demonstrated dynamic total-body PET using ⁶⁸Ga-FAPI-04 in an oncologic setting, showing rapid tracer uptake and a high tracer-to-background ratio (115). Data suggest that total-body modeling is feasible for FAPI ligands, and these promising tracers can also be used to investigate the impact of CVD on fibrotic activity throughout the entire body. With the development of novel antifibrotic treatments (116,117), FAPI PET has the potential to identify suitable subjects by providing insights into the condition of the heart and distant organs. PET radiotracers hold the promise of expediting drug development by facilitating comprehensive

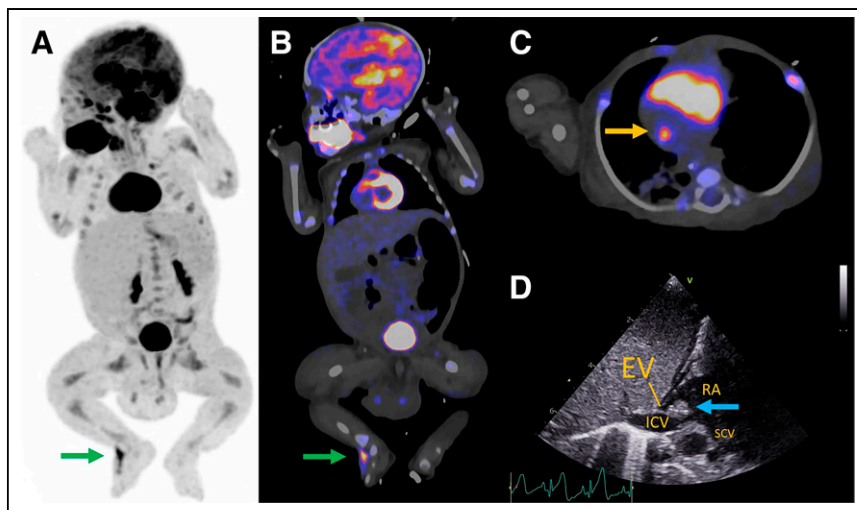


FIGURE 5. 10-wk-old baby presenting with *Staphylococcus aureus* sepsis of unknown origin underwent total-body ^{18}F -FDG PET/CT imaging, which was performed in 3 min (1 bed position) without sedation on Biograph Vision Quadra system (Siemens Healthineers) using only 12 MBq. His medical history consisted of several congenital defects, including Fallot tetralogy and jejunal atresia. Two infectious foci were detected: at dorsum of right foot (A and B, green arrows) around intravenous access line, and at bottom of right atrium near entrance of inferior caval vein (C, arrow). Reactive bone marrow uptake is also visible (A). Ultrasound of foot revealed subcutaneous abscess, which was drained; culturing detected *S. aureus*. ^{18}F -FDG uptake in heart corresponded with solid, echodense structure suggestive of thrombus or vegetation. This is seen on transthoracic echocardiography (D, arrow) at eustachian valve (usually absent by adulthood), indicative of possible endocarditis. Patient improved under antibiotic therapy. (Reprinted with permission of (124).)

assessments. This approach enables (guided) therapy monitoring in total-body mode, encompassing critical aspects such as quantifying receptor occupancy, evaluating drug distribution, conducting pharmacokinetic analyses, confirming target engagement, monitoring treatment responses, and gauging compound concentrations.

The potential extends to understanding the spatial distribution of drugs throughout the entire body, offering insights into how agents accumulate in various tissues over time. Although these dimensions are pivotal in cardiovascular studies, they remain relatively underexplored at present (118).

DISCUSSION

The future of PET is quantitative and, with the availability of the of LAFOV PET/CT systems, represents an exciting development in the field of medical imaging (119). These systems have the potential to not only revolutionize busy clinical services but also enable the investigation of tissue kinetics at multiple levels simultaneously.

From a cardiovascular perspective, this innovative imaging methodology will significantly enhance our understanding of the systemic effects and interactions of various cardiovascular disorders. Until now, these disorders were examined using only single-frame, static, whole-body imaging. In certain cases, imaging at later time points may prove beneficial for achieving a better ratio between the inflammatory lesion and blood-pool activity. For example, it can be useful in conditions such as LVV or cardiac sarcoidosis.

LAFOV PET/CT offers additional advantages such as the ability to perform dynamic scans, which can aid in distinguishing between reactive ^{18}F -FDG uptake and artifact. This feature allows for more accurate visualization of smaller mobile structures in the heart, including suspected endocarditis vegetations, which are frequently missed on conventional PET/CT systems.

Because of the improved sensitivity of a LAFOV PET/CT scanner, scanning even after 4 or 5 half-lives becomes feasible and worth considering. Decreased tracer doses are possible, reducing radiation and creating greater opportunity for serial imaging and therapy monitoring in CVDs. However, the use of CT for attenuation correction in LAFOV PET/CT can contribute significantly to the radiation exposure. Recent CT technology has introduced features such as the tin filter (120) or deep learning algorithms, which can substantially reduce the CT radiation dose (121).

LAFOV PET/CT imaging of multiorgan involvement in several systemic diseases is of potential value, such as in sarcoidosis, amyloidosis, LVV, and atherosclerosis, as PET can be an early marker of systemic disease activity, prevent disease early, better assess prognosis, and determine the optimal moment of therapy induction. Low radiation might also allow (simultaneous) multitracer imaging to assess the link between cardiovascular inflammation and fibroblast activation in these diseases (122). Finally, future research in cardiooncology is an opportunity for LAFOV PET/CT to elucidate the mechanisms involved in cross-talk between cardiac and cancer cells, as cancer cells can promote metabolic remodeling in the heart (123). Metabolic changes provide opportunities for novel treatment strategies to prevent heart failure and monitor disease progression through new imaging techniques. However, along with the opportunities presented by LAFOV PET/CT, there are several challenges that need to be addressed (Table 1).

diac and cancer cells, as cancer cells can promote metabolic remodeling in the heart (123). Metabolic changes provide opportunities for novel treatment strategies to prevent heart failure and monitor disease progression through new imaging techniques. However, along with the opportunities presented by LAFOV PET/CT, there are several challenges that need to be addressed (Table 1).

CONCLUSION

LAFOV PET/CT not only introduces a fast imaging acquisition technique with optimal image quality but also facilitates the implementation of quantitative kinetic imaging in clinical settings. It significantly enhances our knowledge of systemic CVD inter(organ) actions and serves as an excellent method for longitudinal imaging and the serial evaluation of disease activity with time, as well as a method to determine the effectiveness of new medical drugs at the whole-body level.

DISCLOSURE

No potential conflict of interest relevant to this article was reported.

ACKNOWLEDGMENT

We thank Nick van Rijsewijk for the use of Figure 5.

REFERENCES

1. Badawi RD, Shi H, Hu P, et al. First human imaging studies with the EXPLORER total-body PET scanner. *J Nucl Med*. 2019;60:299–303.
2. Slart RH, Tsoumpas C, Glaudemans A, et al. Long axial field of view PET scanners: a road map to implementation and new possibilities. *Eur J Nucl Med Mol Imaging*. 2021;48:4236–4245.

3. van Sluis J, van Snick JH, Brouwers AH, et al. EARL compliance and imaging optimisation on the Biograph Vision Quadra PET/CT using phantom and clinical data. *Eur J Nucl Med Mol Imaging*. 2022;49:4652–4660.
4. van Sluis J, van Snick JH, Brouwers AH, et al. Shortened duration whole body ¹⁸F-FDG PET Patlak imaging on the Biograph Vision Quadra PET/CT using a population-averaged input function. *EJNMMI Phys*. 2022;9:74.
5. Maron DJ, Hochman JS, Reynolds HR, et al. Initial invasive or conservative strategy for stable coronary disease. *N Engl J Med*. 2020;382:1395–1407.
6. Ridker PM, Everett BM, Thuren T, et al. Antiinflammatory therapy with canakinumab for atherosclerotic disease. *N Engl J Med*. 2017;377:1119–1131.
7. Roshandel G, Khoshnia M, Poustchi H, et al. Effectiveness of polypill for primary and secondary prevention of cardiovascular diseases (PolyIran): a pragmatic, cluster-randomised trial. *Lancet*. 2019;394:672–683.
8. Swirski FK, Nahrendorf M. Cardioimmunology: the immune system in cardiac homeostasis and disease. *Nat Rev Immunol*. 2018;18:733–744.
9. Cermakova P, Eriksdotter M, Lund LH, Winblad B, Religa P, Religa D. Heart failure and Alzheimer's disease. *J Intern Med*. 2015;277:406–425.
10. Moslehi JJ. Cardiovascular toxic effects of targeted cancer therapies. *N Engl J Med*. 2016;375:1457–1467.
11. Zannad F, Rossignol P. Cardiorenal syndrome revisited. *Circulation*. 2018;138:929–944.
12. Samsky MD, Patel CB, DeWald TA, et al. Cardiohepatic interactions in heart failure: an overview and clinical implications. *J Am Coll Cardiol*. 2013;61:2397–2405.
13. Oliveira SD. Cardiopulmonary pathogenic networks: unveiling the gut-lung microbiome axis in pulmonary arterial hypertension. *Am J Respir Crit Care Med*. 2023;207:655–657.
14. Tang WH, Kitai T, Hazen SL. Gut microbiota in cardiovascular health and disease. *Circ Res*. 2017;120:1183–1196.
15. Rahmim A, Lodge MA, Karakatsanis NA, et al. Dynamic whole-body PET imaging: principles, potentials and applications. *Eur J Nucl Med Mol Imaging*. 2019;46:501–518.
16. Visvikis D, Lambin P, Beuschau Mauridsen K, et al. Application of artificial intelligence in nuclear medicine and molecular imaging: a review of current status and future perspectives for clinical translation. *Eur J Nucl Med Mol Imaging*. 2022;49:4452–4463.
17. Schindler TH, Bateman TM, Berman DS, et al. Appropriate use criteria for PET myocardial perfusion imaging. *J Nucl Med*. 2020;61:1221–1265.
18. Mielniczuk LM, Toth GG, Xie JX, De Bruyne B, Shaw LJ, Beanlands RS. Can functional testing for ischemia and viability guide revascularization? *JACC Cardiovasc Imaging*. 2017;10:354–364.
19. Mintun MA, Raichle ME, Martin WR, Herscovitch P. Brain oxygen utilization measured with O-15 radiotracers and positron emission tomography. *J Nucl Med*. 1984;25:177–187.
20. Raichle ME, Martin WR, Herscovitch P, Mintun MA, Markham J. Brain blood flow measured with intravenous H₂¹⁵O. II. Implementation and validation. *J Nucl Med*. 1983;24:790–798.
21. Wintermark M, Sesay M, Barbier E, et al. Comparative overview of brain perfusion imaging techniques. *Stroke*. 2005;36:e83–e99.
22. Murthy VL, Bateman TM, Beanlands RS, et al. Clinical quantification of myocardial blood flow using pet: joint position paper of the SNMMI Cardiovascular Council and the ASNC. *J Nucl Med*. 2018;59:273–293.
23. Ngo V, Martineau P, Harel F, Pelletier-Galarneau M. Improving detection of CAD and prognosis with PET/CT quantitative absolute myocardial blood flow measurements. *Curr Cardiol Rep*. 2022;24:1855–1864.
24. Schindler TH, Fearon WF, Pelletier-Galarneau M, et al. Myocardial perfusion PET for the detection and reporting of coronary microvascular dysfunction: a JACC: Cardiovascular Imaging Expert Panel Statement. *JACC Cardiovasc Imaging*. 2023;16:536–548.
25. Juillard L, Janier MF, Fouque D, et al. Dynamic renal blood flow measurement by positron emission tomography in patients with CRF. *Am J Kidney Dis*. 2002;40:947–954.
26. Juillard L, Janier MF, Fouque D, et al. Renal blood flow measurement by positron emission tomography using ¹⁵O-labeled water. *Kidney Int*. 2000;57:2511–2518.
27. Langaa SS, Lauridsen TG, Mose FH, Fynbo CA, Theil J, Bech JN. Estimation of renal perfusion based on measurement of rubidium-82 clearance by PET/CT scanning in healthy subjects. *EJNMMI Phys*. 2021;8:43.
28. Tahari AK, Bravo PE, Rahmim A, Bengel FM, Szabo Z. Initial human experience with rubidium-82 renal PET/CT imaging. *J Med Imaging Radiat Oncol*. 2014;58:25–31.
29. Nitzsche EU, Choi Y, Killion D, et al. Quantification and parametric imaging of renal cortical blood flow in vivo based on Patlak graphical analysis. *Kidney Int*. 1993;44:985–996.
30. Keramida G, Gregg S, Peters AM. Stimulation of the hepatic arterial buffer response using exogenous adenosine: hepatic rest/stress perfusion imaging. *Eur Radiol*. 2020;30:5852–5861.
31. Mossberg KA, Mullani N, Gould KL, Taegtmeier H. Skeletal muscle blood flow in vivo: detection with rubidium-82 and effects of glucose, insulin, and exercise. *J Nucl Med*. 1987;28:1155–1163.
32. Oguro A, Taniguchi H, Koyama H, et al. Quantification of human splenic blood flow (quantitative measurement of splenic blood flow with H₂¹⁵O and a dynamic state method: 1). *Ann Nucl Med*. 1993;7:245–250.
33. Oguro A, Taniguchi H, Koyama H, et al. Relationship between liver function and splenic blood flow (quantitative measurement of splenic blood flow with H₂¹⁵O and a dynamic state method: 2). *Ann Nucl Med*. 1993;7:251–255.
34. Rudroff T, Weissman JA, Bucci M, et al. Positron emission tomography detects greater blood flow and less blood flow heterogeneity in the exercising skeletal muscles of old compared with young men during fatiguing contractions. *J Physiol (Lond)*. 2014;592:337–349.
35. Li EJ, Lopez JE, Spencer BA, et al. Total-body perfusion imaging with [¹¹C]-butanol. *J Nucl Med*. 2023;64:1831–1838.
36. Packard RRS, Votaw JR, Cooke CD, Van Train KF, Garcia EV, Maddahi J. ¹⁸F-flurpiridaz positron emission tomography segmental and territory myocardial blood flow metrics: incremental value beyond perfusion for coronary artery disease categorization. *Eur Heart J Cardiovasc Imaging*. 2022;23:1636–1644.
37. Chou TH, Alvelo JL, Janse S, et al. Prognostic value of radiotracer-based perfusion imaging in critical limb ischemia patients undergoing lower extremity revascularization. *JACC Cardiovasc Imaging*. 2021;14:1614–1624.
38. Suárez C, Zeymer U, Limbourg T, et al. Influence of polyvascular disease on cardiovascular event rates. Insights from the REACH Registry. *Vasc Med*. 2010;15:259–265.
39. Hess CN, Bonaca MP. Contemporary review of antithrombotic therapy in peripheral artery disease. *Circ Cardiovasc Interv*. 2020;13:e009584.
40. Tawakol A, Ishai A, Takx RA, et al. Relation between resting amygdalar activity and cardiovascular events: a longitudinal and cohort study. *Lancet*. 2017;389:834–845.
41. Joshi NV, Vesey AT, Williams MC, et al. ¹⁸F-fluoride positron emission tomography for identification of ruptured and high-risk coronary atherosclerotic plaques: a prospective clinical trial. *Lancet*. 2014;383:705–713.
42. Diekmann J, Koenig T, Zwadlo C, et al. Molecular imaging identifies fibroblast activation beyond the infarct region after acute myocardial infarction. *J Am Coll Cardiol*. 2021;77:1835–1837.
43. Wu M, Ning J, Li J, et al. Feasibility of in vivo imaging of fibroblast activation protein in human arterial walls. *J Nucl Med*. 2022;63:948–951.
44. Tzolos E, Bing R, Andrews J, et al. Noninvasive in vivo coronary artery thrombus imaging. *JACC Cardiovasc Imaging*. 2023;16:820–832.
45. Derlin T, Werner RA, Weiberg D, Derlin K, Bengel FM. Parametric imaging of biologic activity of atherosclerosis using dynamic whole-body positron emission tomography. *JACC Cardiovasc Imaging*. 2022;15:2098–2108.
46. Ebert A, Herzog H, Stocklin GL, et al. Kinetics of 14(R,S)-fluorine-18-fluoro-6-thia-heptadecanoic acid in normal human hearts at rest, during exercise and after dipyridamole injection. *J Nucl Med*. 1994;35:51–56.
47. McArdle B, Dowsley TF, Cocker MS, et al. Cardiac PET: metabolic and functional imaging of the myocardium. *Semin Nucl Med*. 2013;43:434–448.
48. Lopaschuk GD, Ussher JR. Evolving concepts of myocardial energy metabolism: more than just fats and carbohydrates. *Circ Res*. 2016;119:1173–1176.
49. Sörensen J, Harms HJ, Aalen JM, Baron T, Smiseth OA, Flachskampf FA. Myocardial efficiency: a fundamental physiological concept on the verge of clinical impact. *JACC Cardiovasc Imaging*. 2020;13:1564–1576.
50. Gewirtz H. Cardiac PET: a versatile, quantitative measurement tool for heart failure management. *JACC Cardiovasc Imaging*. 2011;4:292–302.
51. Peterson LR, Gropler RJ. Metabolic and molecular imaging of the diabetic cardiomyopathy. *Circ Res*. 2020;126:1628–1645.
52. Kumar V, Hsueh WA, Raman SV. Multiorgan, Multimodality imaging in cardio-metabolic disease. *Circ Cardiovasc Imaging*. 2017;10:e005447.
53. Doehner W, Frenneaux M, Anker SD. Metabolic impairment in heart failure: the myocardial and systemic perspective. *J Am Coll Cardiol*. 2014;64:1388–1400.
54. Lopaschuk GD, Karwi QG, Tian R, Wende AR, Abel ED. Cardiac energy metabolism in heart failure. *Circ Res*. 2021;128:1487–1513.
55. Tuunanen H, Knuuti J. Metabolic remodelling in human heart failure. *Cardiovasc Res*. 2011;90:251–257.
56. Wang G, Nardo L, Parikh M, et al. Total-body PET multiparametric imaging of cancer using a voxelwise strategy of compartmental modeling. *J Nucl Med*. 2022;63:1274–1281.
57. Wang Y, Nardo L, Spencer BA, et al. Total-body multiparametric PET quantification of ¹⁸F-FDG delivery and metabolism in the study of coronavirus disease 2019 recovery. *J Nucl Med*. 2023;64:1821–1830.

58. Birnie DH, Nery PB, Ha AC, Beanlands RS. Cardiac sarcoidosis. *J Am Coll Cardiol*. 2016;68:411–421.
59. Iannuzzi MC, Rybicki BA, Teirstein AS. Sarcoidosis. *N Engl J Med*. 2007;357:2153–2165.
60. Slart RH, Glaudemans A, Lancellotti P, et al. A joint procedural position statement on imaging in cardiac sarcoidosis: from the Cardiovascular and Inflammation & Infection Committees of the European Association of Nuclear Medicine, the European Association of Cardiovascular Imaging, and the American Society of Nuclear Cardiology. *J Nucl Cardiol*. 2018;25:298–319.
61. Dweck MR, Abgral R, Trivieri MG, et al. Hybrid magnetic resonance imaging and positron emission tomography with fluorodeoxyglucose to diagnose active cardiac sarcoidosis. *JACC Cardiovasc Imaging*. 2018;11:94–107.
62. Blankstein R, Osborne M, Naya M, et al. Cardiac positron emission tomography enhances prognostic assessments of patients with suspected cardiac sarcoidosis. *J Am Coll Cardiol*. 2014;63:329–336.
63. Kittleson MM, Maurer MS, Ambardekar AV, et al. Cardiac amyloidosis: evolving diagnosis and management: a scientific statement from the American Heart Association. *Circulation*. 2020;142:e7–e22.
64. Yan J, Planeta-Wilson B, Carson RE. Direct 4-D PET list mode parametric reconstruction with a novel EM algorithm. *IEEE Trans Med Imaging*. 2012;31:2213–2223.
65. Gallegos C, Miller EJ. Advances in PET-based cardiac amyloid radiotracers. *Curr Cardiol Rep*. 2020;22:40.
66. Dhoot GK. Identification and changes in the pattern of expression of slow-skeletal-muscle-like myosin heavy chains in a developing fast muscle. *Differentiation*. 1988;37:53–61.
67. Papathanasiou M, Kessler L, Carpinteiro A, et al. ¹⁸F-flutemetamol positron emission tomography in cardiac amyloidosis. *J Nucl Cardiol*. 2022;29:779–789.
68. Dietemann S, Nkoulou R. Amyloid PET imaging in cardiac amyloidosis: a pilot study using ¹⁸F-flutemetamol positron emission tomography. *Ann Nucl Med*. 2019;33:624–628.
69. Ezawa N, Katoh N, Oguchi K, Yoshinaga T, Yazaki M, Sekijima Y. Visualization of multiple organ amyloid involvement in systemic amyloidosis using ¹¹C-PiB PET imaging. *Eur J Nucl Med Mol Imaging*. 2018;45:452–461.
70. Mestre-Torres J, Lorenzo-Bosquet C, Cuberas-Borros G, et al. Utility of the ¹⁸F-florbetapir positron emission tomography in systemic amyloidosis. *Amyloid*. 2018;25:109–114.
71. Takasone K, Katoh N, Takahashi Y, et al. Non-invasive detection and differentiation of cardiac amyloidosis using ^{99m}Tc-pyrophosphate scintigraphy and ¹¹C-Pittsburgh compound B PET imaging. *Amyloid*. 2020;27:266–274.
72. Trivieri MG, Dweck MR, Abgral R, et al. ¹⁸F-sodium fluoride PET/MR for the assessment of cardiac amyloidosis. *J Am Coll Cardiol*. 2016;68:2712–2714.
73. Perfetto F, Zampieri M, Fumagalli C, Allinovi M, Cappelli F. Circulating biomarkers in diagnosis and management of cardiac amyloidosis: a review for internist. *Intern Emerg Med*. 2022;17:957–969.
74. Tarkin JM, Gopalan D. Multimodality imaging of large-vessel vasculitis. *Heart*. 2023;109:232–240.
75. Dejaco C, Ramiro S, Duftner C, et al. EULAR recommendations for the use of imaging in large vessel vasculitis in clinical practice. *Ann Rheum Dis*. 2018;77:636–643.
76. Slart RH, Writing Group, Reviewer Group, et al. FDG-PET/CT(A) imaging in large vessel vasculitis and polymyalgia rheumatica: joint procedural recommendation of the EANM, SNMMI, and the PET Interest Group (PIG), and endorsed by the ASNC. *Eur J Nucl Med Mol Imaging*. 2018;45:1250–1269.
77. Nielsen BD, Gormsen LC, Hansen IT, Keller KK, Therkildsen P, Hauge EM. Three days of high-dose glucocorticoid treatment attenuates large-vessel ¹⁸F-FDG uptake in large-vessel giant cell arteritis but with a limited impact on diagnostic accuracy. *Eur J Nucl Med Mol Imaging*. 2018;45:1119–1128.
78. Sari H, Mingels C, Alberts I, et al. First results on kinetic modelling and parametric imaging of dynamic ¹⁸F-FDG datasets from a long axial FOV PET scanner in oncological patients. *Eur J Nucl Med Mol Imaging*. 2022;49:1997–2009.
79. Drescher R, Freesmeyer M. PET angiography: application of early dynamic PET/CT to the evaluation of arteries. *AJR*. 2013;201:908–911.
80. Lamare F, Hinz R, Gaemperli O, et al. Detection and quantification of large-vessel inflammation with ¹¹C-(R)-PK11195 PET/CT. *J Nucl Med*. 2011;52:33–39.
81. Nienhuis PH, van Praagh GD, Glaudemans A, Brouwer E, Slart R. A review on the value of imaging in differentiating between large vessel vasculitis and atherosclerosis. *J Pers Med*. 2021;11:236.
82. van der Geest KSM, Sandovici M, Nienhuis PH, et al. Novel PET imaging of inflammatory targets and cells for the diagnosis and monitoring of giant cell arteritis and polymyalgia rheumatica. *Front Med (Lausanne)*. 2022;9:902155.
83. Weber B, Garshick M, Liao KP, Di Carli M. Sore, hot, and at risk: the emerging speciality of cardio-rheumatology. *J Am Heart Assoc*. 2023;12:e027846.
84. Schiattarella GG, Alcaide P, Condorelli G, et al. Immunometabolic mechanisms of heart failure with preserved ejection fraction. *Nat Cardiovasc Res*. 2022;1:211–222.
85. Malhotra S, Fernandez SF, Fallavollita JA, Cauty JM Jr. Prognostic significance of imaging myocardial sympathetic innervation. *Curr Cardiol Rep*. 2015;17:62.
86. Thackeray JT, Bengel FM. Assessment of cardiac autonomic neuronal function using PET imaging. *J Nucl Cardiol*. 2013;20:150–165.
87. Fallavollita JA, Heavey BM, Luisi AJ Jr, et al. Regional myocardial sympathetic denervation predicts the risk of sudden cardiac arrest in ischemic cardiomyopathy. *J Am Coll Cardiol*. 2014;63:141–149.
88. Malhotra S, Singh V, Fallavollita JA, Cauty JM Jr. Myocardial denervation and left ventricular volume predict ventricular arrhythmias in patients with ischemic cardiomyopathy. *JACC Cardiovasc Imaging*. 2022;15:1164–1166.
89. Mu L, Kramer SD, Warnock GI, et al. [¹¹C]mHED PET follows a two-tissue compartment model in mouse myocardium with norepinephrine transporter (NET)-dependent uptake, while [¹⁸F]JLM1195 uptake is NET-independent. *EJNMMI Res*. 2020;10:114.
90. Zelt JGE, Britt D, Mair BA, et al. Regional distribution of fluorine-18-fluorobenguane and carbon-11-hydroxyephedrine for cardiac PET imaging of sympathetic innervation. *JACC Cardiovasc Imaging*. 2021;14:1425–1436.
91. Bengel FM. Imaging targets of the sympathetic nervous system of the heart: translational considerations. *J Nucl Med*. 2011;52:1167–1170.
92. Dutta P, Courties G, Wei Y, et al. Myocardial infarction accelerates atherosclerosis. *Nature*. 2012;487:325–329.
93. Thoonen R, Ermande L, Cheng J, et al. Functional brown adipose tissue limits cardiomyocyte injury and adverse remodeling in catecholamine-induced cardiomyopathy. *J Mol Cell Cardiol*. 2015;84:202–211.
94. DeGrado TR, Hutchins GD, Toorongian SA, Wieland DM, Schwaiger M. Myocardial kinetics of carbon-11-meta-hydroxyephedrine: retention mechanisms and effects of norepinephrine. *J Nucl Med*. 1993;34:1287–1293.
95. Thackeray JT, Beanlands RS, Dasilva JN. Presence of specific ¹¹C-meta-hydroxyephedrine retention in heart, lung, pancreas, and brown adipose tissue. *J Nucl Med*. 2007;48:1733–1740.
96. Grkovski M, Zanzonico PB, Modak S, Humm JL, Narula J, Pandit-Taskar N. F-18 meta-fluorobenzylguanidine PET imaging of myocardial sympathetic innervation. *J Nucl Cardiol*. 2022;29:3179–3188.
97. Udit S, Blake K, Chiu IM. Somatosensory and autonomic neuronal regulation of the immune response. *Nat Rev Neurosci*. 2022;23:157–171.
98. Bin Abdulhak AA, Baddour LM, Erwin PJ, et al. Global and regional burden of infective endocarditis, 1990-2010: a systematic review of the literature. *Glob Heart*. 2014;9:131–143.
99. Morita Y, Haruna T, Haruna Y, et al. Thirty-day readmission after infective endocarditis: analysis from a nationwide readmission database. *J Am Heart Assoc*. 2019;8:e011598.
100. Pant S, Patel NJ, Deshmukh A, et al. Trends in infective endocarditis incidence, microbiology, and valve replacement in the United States from 2000 to 2011. *J Am Coll Cardiol*. 2015;65:2070–2076.
101. Habib G, Badano L, Tribouilloy C, et al. Recommendations for the practice of echocardiography in infective endocarditis. *Eur J Echocardiogr*. 2010;11:202–219.
102. Habib G, Lancellotti P, Antunes MJ, et al. 2015 ESC guidelines for the management of infective endocarditis: the Task Force for the Management of Infective Endocarditis of the European Society of Cardiology (ESC). Endorsed by: European Association for Cardio-Thoracic Surgery (EACTS), the European Association of Nuclear Medicine (EANM). *Eur Heart J*. 2015;36:3075–3128.
103. Lindner JR, Case RA, Dent JM, Abbott RD, Scheld WM, Kaul S. Diagnostic value of echocardiography in suspected endocarditis. An evaluation based on the pretest probability of disease. *Circulation*. 1996;93:730–736.
104. Chen W, Sajadi MM, Dilsizian V. Merits of FDG PET/CT and functional molecular imaging over anatomic imaging with echocardiography and CT angiography for the diagnosis of cardiac device infections. *JACC Cardiovasc Imaging*. 2018;11:1679–1691.
105. Gomes A, Glaudemans A, Touw DJ, et al. Diagnostic value of imaging in infective endocarditis: a systematic review. *Lancet Infect Dis*. 2017;17:e1–e14.
106. Juneau D, Golfam M, Hazra S, et al. Positron emission tomography and single-photon emission computed tomography imaging in the diagnosis of cardiac implantable electronic device infection: a systematic review and meta-analysis. *Circ Cardiovasc Imaging*. 2017;10:e005772.
107. Kim J, Feller ED, Chen W, Liang Y, Dilsizian V. FDG PET/CT for early detection and localization of left ventricular assist device infection: impact on patient management and outcome. *JACC Cardiovasc Imaging*. 2019;12:722–729.
108. Feng T, Zhao Y, Shi H, et al. Total-body quantitative parametric imaging of early kinetics of ¹⁸F-FDG. *J Nucl Med*. 2021;62:738–744.
109. Pijl JP, Kwee TC, Slart R, Yakar D, Wouthuyzen-Bakker M, Glaudemans A. Clinical implications of increased uptake in bone marrow and spleen on

- FDG-PET in patients with bacteremia. *Eur J Nucl Med Mol Imaging*. 2021;48:1467–1477.
110. Roque A, Pizzi MN, Fernandez-Hidalgo N, et al. Mosaic bioprostheses may mimic infective endocarditis by PET/CTA: trust the uptake pattern to avoid misdiagnosis. *JACC Cardiovasc Imaging*. 2020;13:2239–2244.
 111. Scholtens AM, Swart LE, Verberne HJ, Tanis W, Lam MG, Budde RP. Confounders in FDG-PET/CT imaging of suspected prosthetic valve endocarditis. *JACC Cardiovasc Imaging*. 2016;9:1462–1465.
 112. Chen W, Dilsizian V. Molecular imaging of cardiovascular device infection: targeting the bacteria or the host-pathogen immune response? *J Nucl Med*. 2020;61:319–326.
 113. Omidvari N, Jones T, Price PM, et al. First-in-human immunoPET imaging of COVID-19 convalescent patients using dynamic total-body PET and a CD8-targeted minibody. *Sci Adv*. 2023;19:eadh7968.
 114. Ćorović A, Wall C, Nus M, et al. Somatostatin receptor PET/MR imaging of inflammation in patients with large vessel vasculitis and atherosclerosis. *J Am Coll Cardiol*. 2023;81:336–354.
 115. Chen R, Yang X, Yu X, et al. The feasibility of ultra-early and fast total-body [⁶⁸Ga]Ga-FAPI-04 PET/CT scan. *Eur J Nucl Med Mol Imaging*. 2023;50:661–666.
 116. Ishikane S, Arioka M, Takahashi-Yanaga F. Promising small molecule anti-fibrotic agents: newly developed or repositioned drugs targeting myofibroblast transdifferentiation. *Biochem Pharmacol*. 2023;214:115663.
 117. Morfino P, Aimo A, Castiglione V, Galvez-Monton C, Emdin M, Bayes-Genis A. Treatment of cardiac fibrosis: from neuro-hormonal inhibitors to CAR-T cell therapy. *Heart Fail Rev*. 2023;28:555–569.
 118. Ghosh KK, Padmanabhan P, Yang CT, et al. Positron emission tomographic imaging in drug discovery. *Drug Discov Today*. 2022;27:280–291.
 119. Cherry SR, Diekmann J, Bengel FM. Total-body positron emission tomography: adding new perspectives to cardiovascular research. *JACC Cardiovasc Imaging*. 2023;16:1335–1347.
 120. Shiri I, Arabi H, Geramifard P, et al. Deep-JASC: joint attenuation and scatter correction in whole-body ¹⁸F-FDG PET using a deep residual network. *Eur J Nucl Med Mol Imaging*. 2020;47:2533–2548.
 121. Mostafapour S, Greuter M, van Snick JH, et al. Ultra-low dose CT scanning for PET/CT. *Med Phys*. 2024;51:139–155.
 122. Zeng F, Fang J, Muhashi A, Liu H. Direct reconstruction for simultaneous dual-tracer PET imaging based on multi-task learning. *EJNMMI Res*. 2023;13:7.
 123. Karlstaedt A, Barrett M, Hu R, Gammons ST, Ky B. Cardio-oncology: understanding the intersections between cardiac metabolism and cancer biology. *JACC Basic Transl Sci*. 2021;6:705–718.
 124. van Rijsewijk ND, van Leer B, Ivashchenko OV, et al. Ultra-low dose infection imaging of a newborn without sedation using long axial field-of-view PET/CT. *Eur J Nucl Med Mol Imaging*. 2023;50:622–623.